Research Article

Mingrui Du, Yuan Gao, Guansheng Han, Luan Li, and Hongwen Jing*

Stabilizing effect of methylcellulose on the dispersion of multi-walled carbon nanotubes in cementitious composites

https://doi.org/10.1515/ntrev-2020-0009
Received Jun 17, 2019; accepted Nov 05, 2019

Abstract: Multi-walled carbon nanotubes (MWCNTs) have been added in the plain cementitious materials to manufacture composites with the higher mechanical properties and smart behavior. The uniform distributions of MWCNTs is critical to obtain the desired enhancing effect, which, however, is challenged by the high ionic strength of the cement pore solution. Here, the effects of methylcellulose (MC) on stabilizing the dispersion of MWCNTs in the simulated cement pore solution and the viscosity of MWCNT suspensions were studied. Further observations on the distributions of MWCNTs in the ternary cementitious composites were conducted. The results showed that MC forms a membranous envelope surrounding MWCNTs, which inhibits the adsorption of cations and maintains the steric repulsion between MWCNTs; thus, the stability of MWCNT dispersion in cement-based composites is improved. MC can also work as a viscosity adjuster that retards the Brownian mobility of MWCNTs, reducing their re-agglomerate within a period. MC with an addition ratio of 0.018 wt.% is suggested to achieve the optimum dispersion stabilizing effect. The findings here provide a way for stabilizing the other dispersed nano-additives in the cementitious composites.

Keywords: multi-walled carbon nanotubes, methylcellulose, dispersion stability, cementitious composites

1 Introduction

Carbon nanotubes (CNTs), categorized as single-walled carbon nanotubes (SWCNTs) and multi-walled carbon nanotubes (MWCNTs) [1, 2], have low density, superior high aspect ratio and excellent mechanical properties [3, 4]. The tensile strength and Young's modulus of a single MWCNTs was found to be about 11-63 GPa and 270-950 GPa [3]. Due to the excellent material properties, CNTs has found its applications in enhancing various types of composites including organic polymers [5], ceramics [6], and cement-based composites [7–9]. Studies show that the CNTs embedded in cement-based matrices can work as nano-filler as well as play the crack-bridging role [10], and it can improve the load transferring efficiency of the composites through the pulling-out behavior [11]. The enhancement of CNTs at a low addition ratio (<0.5 wt.%) in the cementitious composites has been observed in the strength and stiffness [9, 10, 12]. CNTs, by virtue of the excellent electrical conductivity (>10^3 S/m) [13], has been incorporated in cement-based materials for the resistivity-reducing [14]. In addition, the characteristic of the varied resistivity of the CNTs enhanced cementitious materials versus the external load [15], moisture [16], and chloride concentration [17], providing the composites with the monitoring functions.

To incorporate CNTs properly into cement, their uniform dispersion is required because only the individually distributed CNTs are effective in terms of reinforcement or resistivity decline [7, 18]. The agglomerated CNTs in cement-based materials, however, work as weak spots or introduce defects in the form of voids or unreacted cement particles [18]. Unfortunately, the strong van der Waal's interaction makes the pristine CNTs to attach to each other in bundles or clumps [19]. Preparing the CNTs aqueous suspensions by ultrasonication [7, 18, 20] or high shear treatment [20, 21] is the most used to separate CNTs from agglomerates, at present. Meanwhile, the non-covalently attached surface-active agents (SSAs) that can enhance the steric repulsion between CNTs are generally incorporated for maintaining the stable dispersion of CNTs in aqueous

***Corresponding Author: Hongwen Jing:** State Key Laboratory for Geomechanics & Deep Underground Engineering, China University of Mining & Technology, Xuzhou 221116, China;
Email: jinghwskl@163.com
Mingrui Du: State Key Laboratory for Geomechanics & Deep Underground Engineering, China University of Mining & Technology, Xuzhou 221116, China; School of Water Conservancy Engineering, Zhengzhou University, Zhengzhou 450001, China
Yuan Gao, Guansheng Han, Luan Li: State Key Laboratory for Geomechanics & Deep Underground Engineering, China University of Mining & Technology, Xuzhou 221116, China

Table 1: Structure properties of MWCNTs

Type	Diameter	Length	Specific surface areas	Purity
MWNT-10	5-10 nm	5-15 μm	250-500 m^2/g	> 97%

solutions [18, 19]. Some researchers introduced the covalently attached functional groups like -COOH on the outer walls of MWCNTs to provide the hydrophilicity and repulsion [22]. In fresh cement pastes, more than 95% of CNTs exist in the pore solution which is characterized as a strong Ca^{2+} based alkaline environment (with pH value of higher than 10) [22, 23]. In contrast to the organic solutions [24, 25] and the near neutral aqueous liquid [26], such an alkaline environment is not conductive to the stable CNT dispersion. The dispersion degree of CNTs declines over time at a measurable rate before the hardening of slurries and the CNTs attach to each other; thus, sedimentation of CNT agglomerates happens [23]. It has been reported that after 5 hours, the maximum decline of the dispersion degree can be about 80% [23]. Stabilizing the well-dispersed CNTs in fresh cement is necessary for making full use of their material properties. In previous study [27], methylcellulose (MC), a thickening agent for concrete [28], was found to be helpful in stabilizing the dispersed CNTs in cement pore solution according to the UV-vis-NIR test results. In Ref. [27], it was found that at 4 h, the MWCNT suspension with 0.18 wt.% MC had about 51% of dispersed MWCNTs, which was almost double of the amount of MWCNTs in suspension without MC. MC, on the other hand, is also helpful for avoiding the precipitation of cement particles during the hardening process. The bleeding rate of the fresh pastes was lower than 4.0% when 0.10 wt.% MC was incorporated. However, in Ref. [27], researchers have focused on the influences of MC on the fluidity, porosity, compressive strength and elastic modulus of the CNTs enhanced cementitious composites, whereas the interactions between MC and CNTs, and the distribution of CNTs in the composites are neglected. Little information about the exact role of MC in the mixtures has been provided. Understanding of the working mechanism of MC on stabilizing the well-separated CNTs in cementitious materials requires further research.

Here, the stabilizing effects of different dosages of MC on the dispersion of MWCNTs in the simulated cementitious pore solution were identified by measuring the Zeta potential of MWCNT suspensions and the hydrodynamic diameter of the agglomerates [22]. Influences of MC on the viscosity of MWCNT suspensions were tested. Distributions of MWCNTs in the pore solution and in cement were visually observed using TEM (transmission electron microscopy) and SEM (scanning electron microscopy), respectively. This study shows MC, with a moderate addition, can forms a membranous envelope surrounding MWCNTs that inhibits the adsorption of cations, thus maintaining the steric repulsion, and works as viscosity modifier that retards the Brownian mobility of MWCNTs, which enhance the resistance of MWCNTs to the re-agglomeration within a period. Findings provide a method for maintaining the stable dispersion of other nano-additives in alkaline cementitious environments.

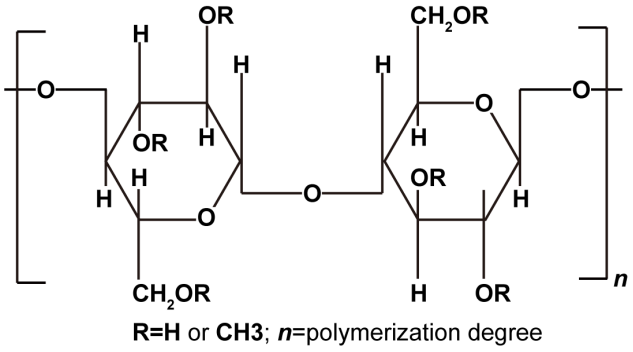

Figure 1: The chemical elements and structure of MC

2 Experimental process

2.1 Raw materials and instrumentation

The structure properties of the non-functionalized MWCNTs used here are presented in Table 1. The polycarboxylate-based superplasticizer (PC) was used as SSA for dispersing the MWCNTs. Methylcellulose (MC) was adopted for stabilizing MWCNTs. The representation of chemical elements and structure of MC are shown in Figure 1. Portland cement (OPC, P.O. 42.5), silica fume (SF) and fly ash (FA) were adopted to prepare the cementitious blends. FA and SF were added to obtain a more general cementitious composite [29, 30]. The addition of FA and SF allows the use of less amount of cement and thus decreases the associated carbon dioxide emission and reduces the potential economic cost [31, 32].

A horn ultra-sonicator with a cylindrical tip, SONICS VCX 500W, was used to separate the MWCNTs in distilled

water. The end-cap diameter of the sonicator tip is 13 mm. A zeta potential analyzer, NanoBrook 90 Plus was used to measure the Zeta potential of suspensions and the hydrodynamic size (***D***) of nanoparticles. The morphology of MWCNT bundles in the simulated cement pore solutions was visually characterized using TEM (Tecnai G2 F20). A digital rotary viscometer, type NDJ-9S was used to measure the coefficient of viscosity ($\boldsymbol{\mu}$) of the MWCNT suspensions that contains different content of MC. The embedded MWCNTs in the hardened matrix was observed using SEM (HITACHI SU8220).

2.2 Fabrication of MC-MWCNT suspensions

With the pulse ultrasonic method, MWCNTs were separated in the PC aqueous solutions under ultra-sonication for producing the uniform MWCNT suspensions. The ultrasonic process lasted for 12 min and about 750 J/mL ultrasonication energy was input into the mixtures. The water-ice bath treatment was used during sonication to prevent the overheating of the mixtures. Then, MC was dissolved into the suspensions by stirring at a rate of 200 rpm for about 10 min. MC was infiltrated by ethanol to accelerate its dissolution. The mixtures were left for 120 min to until the bubbles disappeared before the subsequent experiments. The mass concentrations of MWCNTs, PC, and MC in the suspensions are shown in Table 2. The weight of PC was about eight times that of MWCNTs, as suggested in the literature [10]. Five groups of MC-MWCNT suspensions MC were prepared.

Table 2: Mass concentrations of MWCNTs, PC and MC in the prepared MC-MWCNT suspensions

Suspensions	C/s (wt.%)	P/s (wt.%)	MC/s (wt.%)
MC-0	0.08	0.64	0.00
MC-1			0.18
MC-2			0.35
MC-3			0.70
MC-4			1.00

Note: C/s, P/s and MC/s represent the weight percentages of MWCNTs, PC and MC to the suspensions

2.3 Dispersion and viscosity tests of the MC-MWCNT suspensions

A simulated cement pore solution, with the chemical concentrations suggested in Refs was firstly prepared to obtain the alkaline cementitious environment [23, 33]. Then, MC-MWCNT suspensions were diluted to 1/50 of their initial concentrations with the pore solution for simulating introducing MWCNTs into cement. Zeta potential of the MC-MWCNT suspensions and the hydrodynamic size (***D***) of nanoparticles were measured to characterize the dispersion degree of MWCNTs in this environment. Volumes (3 mL) of the mixtures were stored in phials and transferred to the zeta-potential analyzer. The variations of Zeta potential and ***D*** every 30 min for 4 h were measured. All suspensions were equilibrated for 2 min at room temperature before the measurements. To confirm the reproducibility, two samples were prepared for each group of suspensions for the measurement of Zeta potential and ***D***.

The diluted suspensions were stored in phials for visual observation. And at the times of 0, 60 min, 120 min and 240 min after dilution, a drop of liquid was dropped on the copper grid and dried in room temperature for investigating the morphology of the MWCNT agglomerates. Only the MWCNT agglomerates in the suspensions MC-0, MC-1 and MC-4 were observed by TEM. During the dispersion testing process, the coefficient of viscosity ($\boldsymbol{\mu}$) of the diluted MC-MWCNT suspensions was tested simultaneously. The rotation speed was fixed at 6 rpm and the No. 0 rotor was adopted. Three samples for each group of suspensions were prepared for the viscosity measuring.

2.4 Distributions of MWCNTs in cement-based matrixes

The distributions of MWCNTs in the hardened cement-based matrixes were observed by SEM. Suspensions MC-1, MC-2, and MC-4 were used to make the MWCNTs enhanced cementitious composites. Suspensions were added into the mixed ternary powders containing OPC, SF, and FA. The mass contents of OPC, SF and FA were 80%, 10% and 10%, respectively, as suggested in literature [29, 30]. The water to powder ratio (w/c) of the slurries was 0.6. Such a high or higher w/c is often used to prepare the high-fluidity cementitious materials [31]. More details about the fabrication of the pastes and the curing conditions are included in Ref. [27]. In order to reveal the MWCNTs covered by the C-S-H gels or other hydration products [34], before the SEM investigation, the hardened composites were treated with the acid etching. To be exact, matrixes were immersed in

the hydrochloric acid with pH of 4 for half a minute for dissolving the hydration products, and then rinsed in ultrapure water for the acid residue removing. With the dilution acid and the limited etching time, the influences of etching on the distributions of MWCNT could be ignored.

3 Results and discussion

3.1 Effects of MC on the dispersion of MWCNTs in pore solution

The variations of Zeta potential of MC-MWCNT suspensions versus time are shown in Figure 2. The Zeta potential of the suspensions decreased gradually with the increasing storage time, indicating the decreased dispersion stability of MWCNTs in the pore solution [22]. After about 1 hour and a half, the Zeta potential of all the suspensions was with values of over 12 mV. The suspension MC-1 showed the highest Zeta potential value, then the suspension MC-2, implying these suspensions have higher dispersion degree of MWCNTs than other suspensions [22].

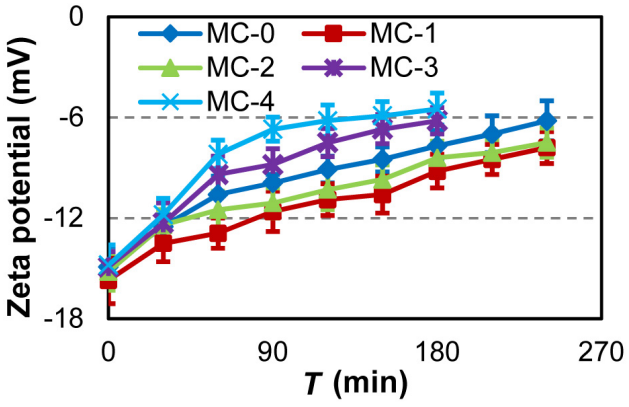

Figure 2: Zeta potential of the MC-MWCNT suspensions at different storage time

Figures 3 (a)-(e) show the probability distributions of $\boldsymbol{D}$ of nanoparticles in MC-MWCNT suspensions at different storage time. For the suspensions MC-0 and MC-1, with the increasing storage time, the peaks of the probability curves of log($\boldsymbol{D}$) move to the right and the probability curves become gradually wider, which is mainly caused by the increasing amount of the re-agglomerated MWCNTs. Compared to the suspension MC-0, the increasing trend of $\boldsymbol{D}$ of the agglomerates in the suspension MC-1 is slower, indicating that MC can effectively restrain the re-agglomeration of MWCNTs. As for the suspension MC-4, the probability curves of log($\boldsymbol{D}$) vary in a similar way in the first 60 min, after which the peaks of the probability curves shift to the left. This is mainly because a large amount of MWCNT agglomerates have settled to the bottom (Figure 3(f)), and the amount of the small agglomerates of MWCNTs remaining in the suspensions reduce, giving rise to the decreased size of the agglomerated nanoparticles.

Based on the probability curves of $\boldsymbol{D}$, $\boldsymbol{D_0}$ and $\boldsymbol{D_T}$, the average $\boldsymbol{D}$ of nanoparticles at the initial time and a specific time $\boldsymbol{T}$ can be calculated, and $\boldsymbol{D_T/D_0}$, the relative increase of the average $\boldsymbol{D}$ of the MWCNT agglomerates, can be obtained. The variations of $\boldsymbol{D_T/D_0}$ for different MC-MWCNT suspensions are presented in Figure 4.

Figure 4 demonstrates that $\boldsymbol{D_T/D_0}$ of all the MC-MWCNT suspensions is higher than 1.0 and presents an increasing trend over time until a plateau is achieved, except for suspension MC-4. The sedimentation phenomenon of the re-agglomerated MWCNTs was more significant in suspension MC-4 (Figure 3 (f)). The continuously increasing $\boldsymbol{D_T/D_0}$ illustrates the progressive agglomeration of MWCNTs over time. Suspensions with MC ratios of 0.18 wt.% and 0.35 wt.% are found to perform better in stabilizing the dispersion of MWCNTs, as their $\boldsymbol{D_T/D_0}$ values are always lower than those of other suspensions, a finding consistent with the reported results of absorbance in Ref. [27]. In addition, Figure 4 clearly demonstrates that the slope of the curve of $\boldsymbol{D_T/D_0}$ at the increase stage declines with the increasing concentrations of MC until MC/s reaches 0.70 wt.%. Moreover, the $\boldsymbol{D_T/D_0}$ of suspensions with MC/s of 0.70 wt.%, 1.00 wt% can be higher than that of suspension MC-0 before sedimentation.

All the observations on the variations of Zeta potential and hydrodynamic size imply that an appropriate amount of MC is required to stabilize the dispersed MWCNTs, and excess MC accelerates the sedimentation of MWCNTs in cement pore solution. Adding 0.018-0.036 wt% of MC is preferred to give the favorable stabilizing effect.

3.2 TEM investigations on the distribution of MWCNTs in pore solutions

Figure 5 presents the investigated morphology of MWCNTs agglomerates in cement pore solutions at different time. More TEM results are covered in Figure S1. The observed regions were randomly chosen.

Figure 5 (a) shows that the matter in the suspensions start to adsorb and accumulate on the surface of individual MWCNTs immediately after mixing. The amount of the accumulated microparticles on MWCNTs was more and more, and the MWCNTs tended to connect to each other. About

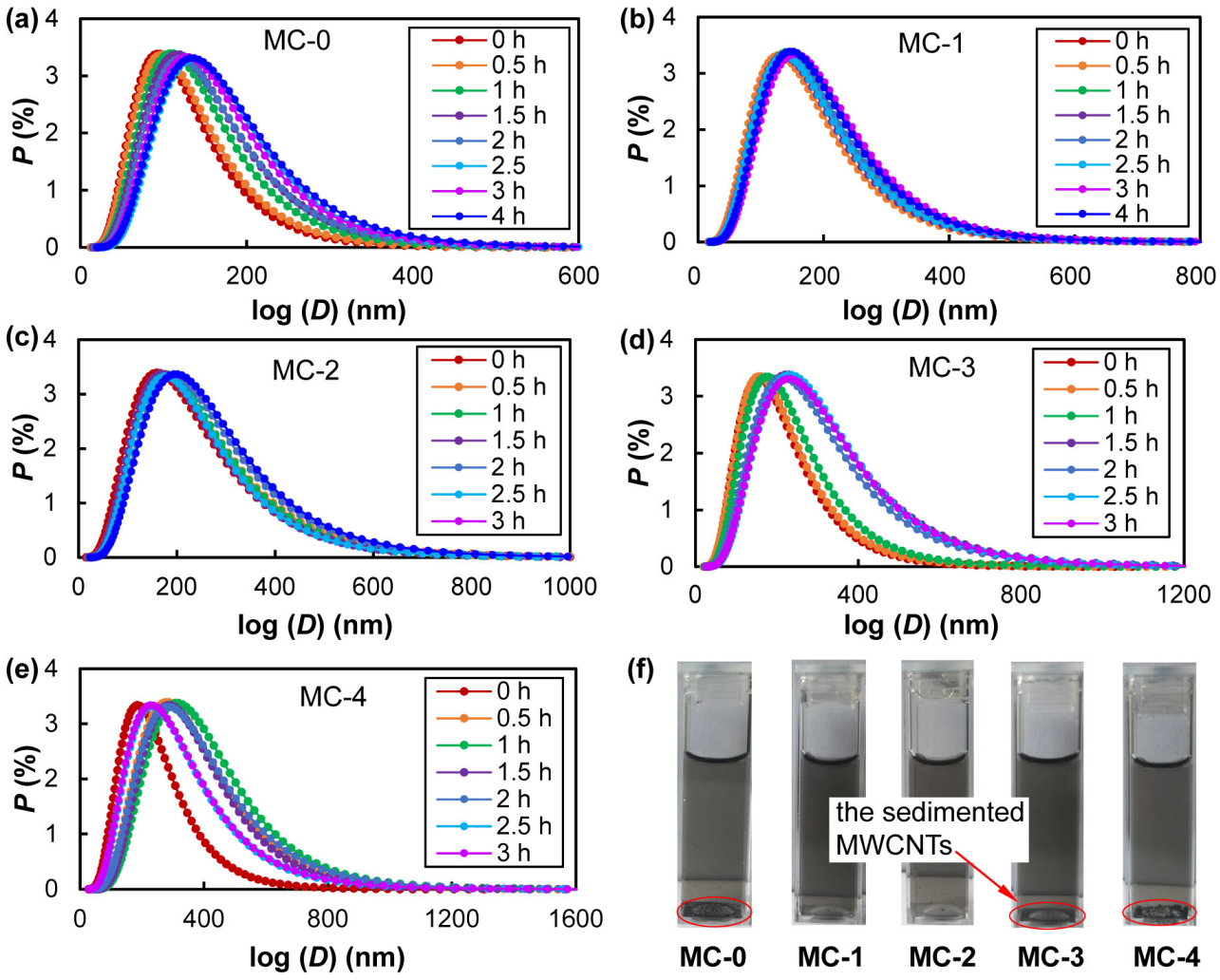

Figure 3: (a)-(e) Probability of log(***D***) of nanoparticles in the MC-MWCNT suspensions, (f) visual observation results of the MC-MWCNT suspensions after 120 min

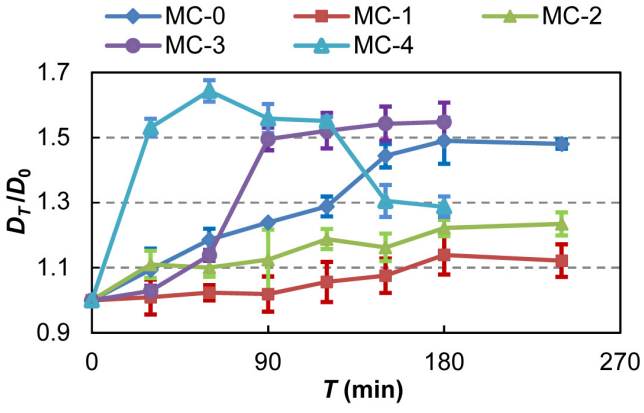

Figure 4: Variations of D_T/D_0 for different MC-MWCNT suspensions versus time; error bars indicate one standard deviation

4 h later, the netlike agglomerates of MWCNTs formed. Figure 5 (b) shows that the molecular MC could form a layer of a membrane-like structure that wraps the individual MWCNTs to protect them effectively from the adsorption of solute. After 120 min, the amount of microparticles surrounding the MWCNTs was much lower. 4 hours later, re-agglomerated MWCNTs could be found as well, but with a smaller volume, corresponding well with the results presented in Figure 4. When an excess amount of MC was added, the netlike MWCNT agglomerates were observed from the beginning time (Figure 5 (c)). After 60 min, most of the MWCNTs appeared in an interwoven form or in clumps. The clumped MWCNTs were stilled wrapped by MC. As most of the MWCNTs appeared in the agglomeration in the suspension MC-4 after about 1 hour, therefore, no TEM images were taken anymore in the following time.

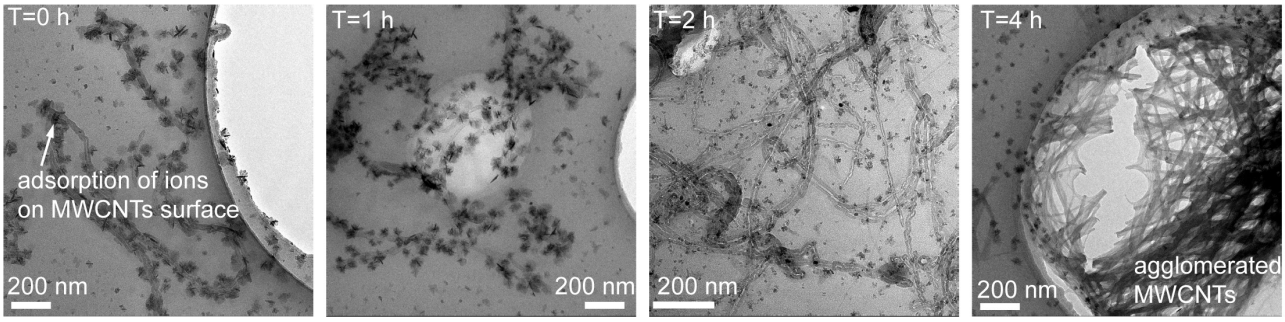

(a) MC-0

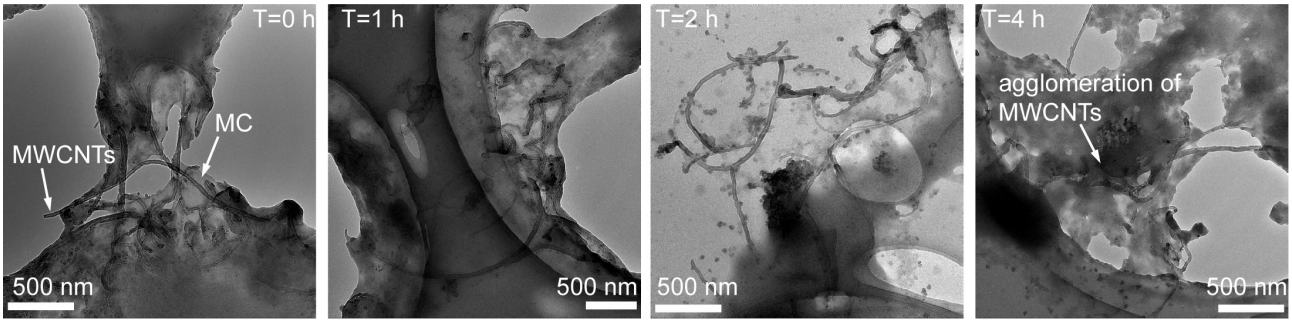

(b) MC-1

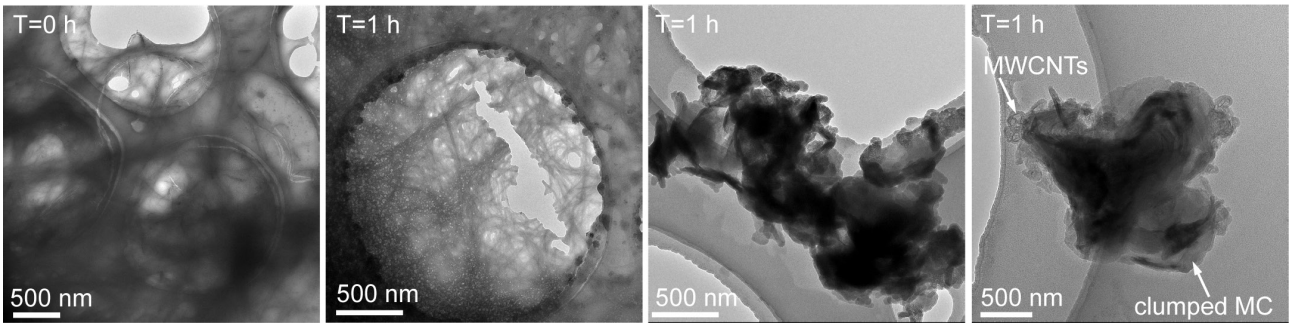

(c) MC-4

Figure 5: TEM images of MWCNTs agglomerates in pore solution at different time

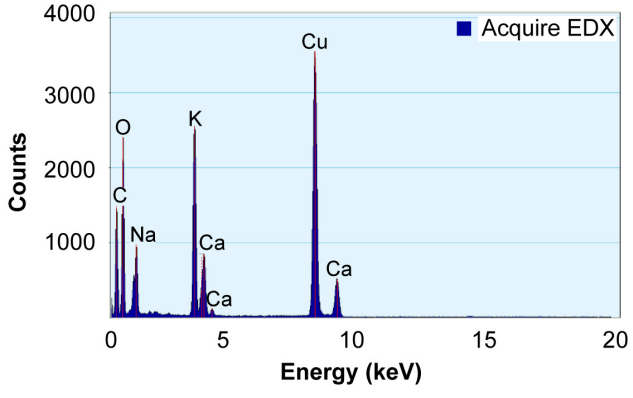

Figure 6: EDX analysis results of the MC-MWCNT suspension (MC-0)

Figure 6 demonstrates the Energy Dispersive X-Ray Spectroscopy (EDX) result of the agglomerated particles observed in suspension MC-0 after mixing. The resource of copper (Cu) here is the copper grid substrate. The carbon (C) was provided by MWCNTs and the oxygen (O) came from the impurities in MWCNTs. Thereby, both the sodium (Na), potassium (K) and calcium (Ca) should be the constituents of the microparticles surrounding MWCNTs, and they came from the pore solutions, indicating that the cationic (Ca^{2+}, K^{+}, Na^{+}) in the pore solutions will adsorb on the surface of the individual MWCNTs after mixing. In MWCNT aqueous suspensions, molecular PC can wrap onto the surface of the MWCNTs via the hydrophobic groups, whereas the hydrophilic parts are pointed outwards, making the MWCNTs disperse well through steric

interaction [19]. The adsorption of ions will lower the surface potential of the dispersed MWCNTs and decline the steric repulsion, resulting in the re-attachment of MWCNTs (Figure 5 (a)) [23]. With the existence of the MC membrane, the adsorption of ions can be inhibited effectively (Figure 5 (b)); thus, the re-agglomeration of MWCNTs in the cement pore solutions can be retarded. However, at higher concentration, the MC chains are more readily to connect into a network that can link the MWCNTs into the large agglomerations (Figure 5 (c)) [35].

3.3 Effect of MC on the viscosity of MC-MWCNT suspensions

Figure 7 shows the viscosity measurement results of MC-MWCNT suspensions with different mass contents of MC. Figure 7 shows that $\boldsymbol{\mu}$ of the MC-MWCNT suspensions increases significantly with increasing dosages of MC. The maximum increase in $\boldsymbol{\mu}$ can be higher than 600%. Since the averaged $\boldsymbol{\mu}$ value of a MWCNT suspension with no MC is about 1 mPa·s, very close to that of pure water (0.9 mPa·s), the higher value of $\boldsymbol{\mu}$ is caused mainly by the addition of MC.

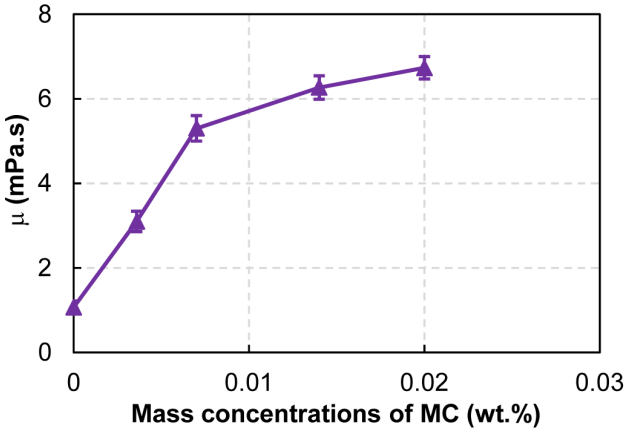

Figure 7: Variations of μ of the diluted MC-MWCNT suspensions versus mass content of MC. Error bars indicate one standard deviation

MC, a long-chain substituted cellulose, is a typical non-ionic water-soluble polymer [36]. The diluted molecular MC in the suspensions spreads out and the free movement of molecular water will be restrained [28]. Therefore, the viscosity of the suspensions is increased. Brownian motion is a physical process that the suspended microscopic particles in liquids or gases move randomly and it is resulted from the impact of molecules of the surrounding mediums [37]. Owing to the small size characteristic of MWCNTs (Table 1), the potentially effect of Brownian motion on the MWCNT aggregation should not be discounted [38]. The aggregation of MWCNTs is an assembly process of the singly distributed fibers that influenced by the inter-particle separation [38]. Assuming the equidistantly separated MWCNTs, over a period of time, the longer the mean travel distance of MWCNTs, the more likely the nanoparticles are to agglomerate. Studies [39] have pointed out that the mean travel distance of particles declines logarithmically versus the increasing viscosity of surrounding medium. That is to say, the intensity of Brownian motion is negatively influenced by the increasing viscosity. From this perspective, in suspensions containing a moderate amount of MC, the non-interacting nanotubes have the deficient Brownian motion to re-agglomerate over a period of time [40, 41]. Namely, MWCNTs can be remained separately within the time period. Therefore, MC also helps to avoid the re-aggregation of MWCNTs via viscosity modifying effect.

3.4 Distributions of MWCNTs in cement matrixes

The SEM observation results of the distribution of MWCNTs in cement-based composites are presented in Figure 8. More SEM observation results can be found in Figure S2. All the SEM images were randomly taken on the samples.

As shown in Figure 8 (a), when the cement-based composites were manufactured without adding any MC, MWCNTs in the matrix were in clumps, whereas MWCNTs were more likely to be embedded in the matrix as single fibers or in the separated state when moderate amount of MC (with *MC*/*s* of 0.18 wt.% and 0.35 wt.%) was used (Figure 8 (b), (c)). For the composites prepared by adding suspension MC-4, as presented in Figures 8 (d) and (e), the MWCNTs in the hardened matrixes were more likely to be in clumps or agglomerations. More details can be found in Figure 8 (f) to (h). The distributions of MWCNTs in cement-based matrixes is very consistent with the dispersion test results (Section 3.1), showing that moderate additions of MC to MWCNT suspensions can improve the dispersion degree of nanotubes in cement pastes, which benefits the uniform distribution of MWCNTs in cement-based matrixes. The more uniformly embedded MWCNTs in the hardened composites can play their role in strength enhancement much better, which has been experimentally verified. In Ref. [27], authors have reported that adding 0.018 wt% MC to the MWCNT suspensions achieves the maximum enhancing efficiency of MWCNTs on the strength and stiffness of the cementitious composites. The maximum increase in the

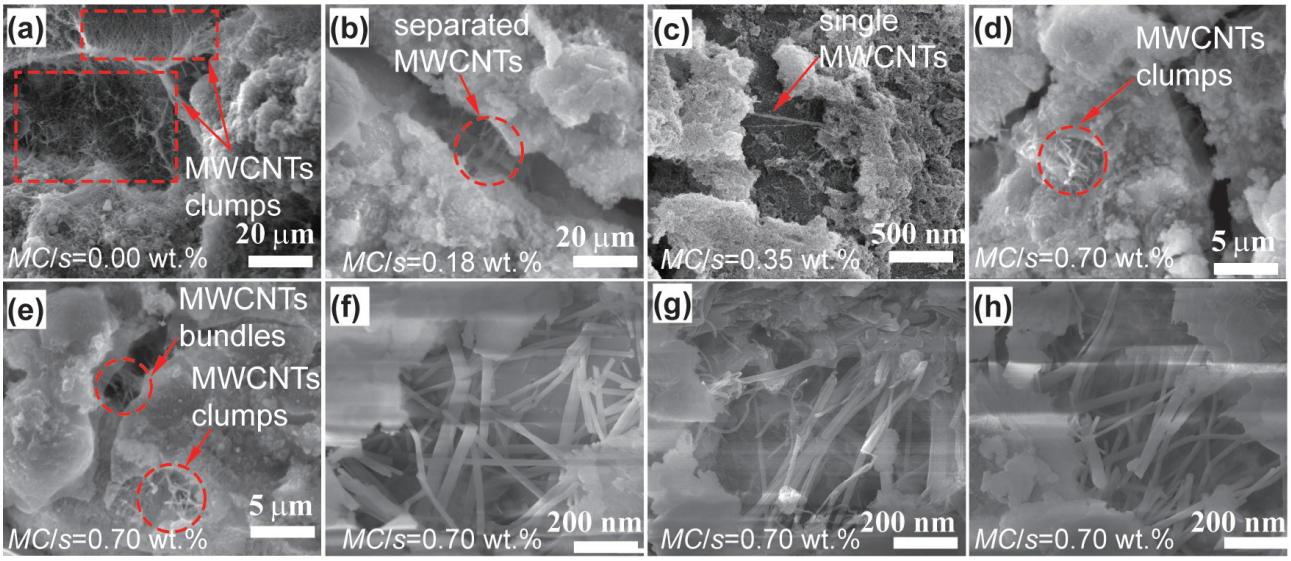

Figure 8: MWCNTs embedded in the ternary cementitious materials

peak uniaxial compression stress was about 16%, whereas the MWCNT-enhanced cementitious materials containing other contents of MC obtained about 3-10% increase in the compression strength.

Moreover, in addition to the CNTs, other nanomaterials, such as carbon nanofibers [42, 43], graphene [44, 45], graphene oxide [46–48], and boron nitride [49], have been incorporated to make high-strength cementitious materials. The dispersion of all these nanomaterials in the cement environment is challenging. The findings here provide a new way to stabilize the dispersion of nanoscale additives in cementitious materials. In addition, MC is nontoxic and it has good compatibility with cementitious materials [28]. Even there is a trade-off between fluidity and stability when MC is used, the thickening effect of MC that helps to prevent the separation of water and cement grains allows the use of less cement when an appropriate mixing rate is adopted [27], which can be cost-saving, eco-friendly and beneficial especially for the cementitious materials with high water content.

4 Conclusions

Here, the role of MC on stabilizing the dispersion of MWCNT in simulated cementitious pore solution was studied, and distribution of MWCNTs in the cementitious composites was investigated. The following conclusions can be drawn:

1. In MWCNT suspensions, molecular MC can form a membrane that wraps MWCNTs. The MC membrane can protect the well-dispersed MWCNTs from the adsorption of ions in cementitious pore solution, which helps to maintain the steric interaction and retards the re-agglomeration. However, at higher concentration, the connected MC chains can link the adjacent MWCNTs into a large gel, accelerating the formation of MWCNT agglomerates.
2. The addition of MC can increase the viscosity of MC-MWCNT suspensions. This also contributes to the stable dispersion of MWCNTs since the higher viscosity gives the individual carbon nanotubes insufficient Brownian motion ability to re-agglomerate within a period.
3. The SEM images show that MWCNTs are more likely to distribute individually in the cement-based matrixes with a moderate addition of MC, whereas the nanotubes appeared in clumps or agglomerates when excess MC is incorporated. A content of 0.018 wt% MC is preferred to give the optimum dispersion results.

Acknowledgement: This study was supported by “the Fundamental Research Funds for the Central Universities [2017BSCXA22]” and “Graduate student scientific research innovation projects in Jiangsu province [KYCX17_1529]”.

References

[1] Iijima S., Helical microtubules of graphitic carbon, Nature, 1991, 354(6348), 56-58.

[2] Ajayan P.M., Nanotubes from Carbon, Chem Rev., 1999, 99(7), 1787-1800.
[3] Yu M.F., Lourie O., Dyer M.J., Moloni K., Kelly T.F., Ruoff R.S., Strength and Breaking Mechanism of Multiwalled Carbon Nanotubes under Tensile Load, Science, 2000, 287(5453), 637-640.
[4] Duan W.H., Wang Q., Liew K.M., He X.Q., Molecular mechanics modeling of carbon nanotube fracture, Carbon, 2007, 45(9), 1769-1776.
[5] Coleman J.N., Khan U., Blau W.J., Gun'Ko Y.K., Small but strong: A review of the mechanical properties of carbon nanotube–polymer composites, Carbon, 2006, 44(9), 1624-1652.
[6] Gao C.D., Pei F., Peng S.P., Shuai C., Carbon nanotube, graphene and boron nitride nanotube reinforced bioactive ceramics for bone repair, Acta Biomater., 2017, 61, 1-20.
[7] Chen S.J., Collins F.G., Macleod A.J.N., Pan Z., Duan W.H., Wang C.M., Carbon nanotube–cement composites: A retrospect, IES J. Part A Civ. Struct. Eng., 2011, 4(4), 254-265.
[8] Li G.Y., Wang P.M., Zhao X.H., Mechanical behavior and microstructure of cement composites incorporating surface-treated multi-walled carbon nanotubes, Carbon, 2005, 43(6), 1239-1245.
[9] Musso S., Tulliani J.M., Ferro G., Tagliaferro A., Influence of carbon nanotubes structure on the mechanical behavior of cement composites, Compos. Sci. Technol., 2009, 69(11), 1985-1990.
[10] Zou B., Chen S.J., Korayem A.H., Collins F., Wang C.M., Duan W.H., Effect of ultrasonication energy on engineering properties of carbon nanotube reinforced cement pastes, Carbon, 2015, 85, 212-220.
[11] Parveen S., Rana S., Fangueiro R., A review on nanomaterial dispersion, microstructure, and mechanical properties of carbon nanotube and nanofiber reinforced cementitious composites, J. Nanomater., 2013, 2013(7), 80.
[12] Xu S.L., Liu J.T., Li Q.H., Mechanical properties and microstructure of multi-walled carbon nanotube-reinforced cement paste, Constr. Build. Mater., 2015, 76, 16-23.
[13] Ebbesen T.W., Lezec H.J., Hiura H., Bennett J.W., Ghaemi H.F., Thio T., Electrical conductivity of individual carbon nanotubes, Nature, 1996, 382(6586), 54-56.
[14] Yoo D.Y., You I., Lee S.J., Electrical Properties of Cement-Based Composites with Carbon Nanotubes, Graphene, and Graphite Nanofibers, Sensors, 2017, 17(5), 1064-1076.
[15] Konsta-Gdoutos M.S., Aza C.A., Self sensing carbon nanotube (CNT) and nanofiber (CNF) cementitious composites for real time damage assessment in smart structures, Cem. Concr. Compos., 2014, 53, 162-169.
[16] Jang S.H., Hochstein D.P., Kawashima S., Yin H., Experiments and micromechanical modeling of electrical conductivity of carbon nanotube/cement composites with moisture, Cem. Concr. Compos., 2017, 77, 49-59.
[17] Kim H.K., Chloride penetration monitoring in reinforced concrete structure using carbon nanotube/cement composite, Constr. Build. Mater., 2015, 96, 29-36.
[18] Collins F., Lambert J., Duan W.H., The influences of admixtures on the dispersion, workability, and strength of carbon nanotube–OPC paste mixtures, Cem. Concr. Compos., 2012, 34(2), 201-207.
[19] Sobolkina A., Mechtcherine V., Khavrus V., Maier D., Mende M., Ritschel M., Leonhardt A., Dispersion of carbon nanotubes and its influence on the mechanical properties of the cement matrix, Cem. Concr. Compos., 2012, 34(10), 1104-1113.
[20] Zhu P., Deng G.S., Shao X.D., Review on Dispersion Methods of Carbon Nanotubes in Cement-based Composites, Mater. Rev., 2018, 32(1), 149-166.
[21] Xu G.H., Zhang Q., Huang J.Q., Zhao M.Q, Zhou W.P., Wei F., A two-step shearing strategy to disperse long carbon nanotubes from vertically aligned multiwalled carbon nanotube arrays for transparent conductive films, Langmuir, 2010, 4(26), 2798-2804.
[22] Chen S.J., Qiu C.Y., Korayem A.H., Barati M.R., Duan W.H., Agglomeration process of surfactant-dispersed carbon nanotubes in unstable dispersion: A two-stage agglomeration model and experimental evidence, Powder Technol., 2016, 301, 412-420.
[23] Chen S.J., Wang W., Sagoe-Crentsil K., Collins F., Zhao X.L., Majumder M., Duan W.H., Distribution of carbon nanotubes in fresh ordinary Portland cement pastes: understanding from a two-phase perspective, RSC Adv., 2016, 6(7), 5745-5753.
[24] Pircheraghi G., Foudazi R., Manas-Zloczower I., Characterization of carbon nanotube dispersion and filler network formation in melted polyol for nanocomposite materials, Powder Technol., 2015, 276, 222-231.
[25] Jia X.L., Zhang Q., Huang J.Q., Zheng C., Qian W.Z., Wei F., The direct dispersion of granular agglomerated carbon nanotubes in bismaleimide by high pressure homogenization for the production of strong composites, Powder Technol., 2012, 217, 477-481.
[26] Munkhbayar B., Nine M.J., Jeoun J., Bat-Erdene M., Chung H., Jeong H., Influence of dry and wet ball milling on dispersion characteristics of the multi-walled carbon nanotubes in aqueous solution with and without surfactant, Powder Technol., 2013, 234, 132-140.
[27] Du M.R., Jing H.W., Duan W.H., Han G.H., Chen S.J., Methylcellulose stabilized multi-walled carbon nanotubes dispersion for sustainable cement composites, Constr. Build. Mater., 2017, 146, 76-85.
[28] Fu X.L., Chung D.D.L., Effect of methylcellulose admixture on the mechanical properties of cement, Cem. Concr. Res., 1996, 26(4), 535-538.
[29] Shehata M.H., Thomas M.D.A., Use of ternary blends containing silica fume and fly ash to suppress expansion due to alkali–silica reaction in concrete, Cem. Concr. Res., 2002, 32(3), 341-349.
[30] Radlinski M., Olek J.. Investigation into the synergistic effects in ternary cementitious systems containing portland cement, fly ash and silica fume, Cem. Concr. Compos., 2012, 34(4), 451-459.
[31] Mirza J., Mirza M.S., Roy V., Saleh K., Basic rheological and mechanical properties of high-volume fly ash grouts, Constr. Build. Mater., 2002, 16(6), 353-363.
[32] Mehta P.K., Gjørv O.E., Properties of portland cement concrete containing fly ash and condensed silica-fume, Cem. Concr. Res., 1982, 12(5), 587-595.
[33] Rajabipour F., Sant G., Weiss J., Interactions between shrinkage reducing admixtures (SRA) and cement paste's pore solution, Cem. Concr. Res., 2008, 38(5), 606-615.
[34] Du M.R., Chen S.J., Duan W.H., Chen W.Q., Jing H.W., Role of Multi-Walled Carbon Nanotubes as Shear Reinforcing Nano-pins in Quasi-Brittle Matrices, ACS Appl. Nano Mater., 2018, 1(4), 1731-1740.
[35] Nasatto P., Pignon F., Silveira J., Duarte M.E., Noseda M., Rinaudo M., Methylcellulose, a Cellulose Derivative with Original Physical Properties and Extended Applications, Polymers, 2015, 7(5): 777-803.
[36] Haque A., Richardson R.K., Morris E.R., Gidley M.J., Caswell D.C., Thermogelation of methylcellulose. Part II: effect of hydroxypropyl substituents, Carbohydr. Polym., 1993, 22(3), 175-186.

[37] Jang S., Choi S., Role of Brownian Motion in the Enhanced Thermal Conductivity of Nanofluids, Appl. Phys. Lett., 2004, 84, 4316-4318.
[38] Osazuwa O., Kontopoulou M., Xiang P., Ye Z., Docoslis A., Electrically conducting polyolefin composites containing electric field-aligned multiwall carbon nanotube structures: The effects of process parameters and filler loading, Carbon, 2014, 72, 89-99.
[39] Monti M., Natali M., Torre L., Kenny J.M., The alignment of single walled carbon nanotubes in an epoxy resin by applying a DC electric field, Carbon, 2012, 50(7), 2453-2464.
[40] Huang Y.Y., Terentjev E.M., Dispersion of Carbon Nanotubes: Mixing, Sonication, Stabilization, and Composite Properties, Polymers, 2012, (4), 275-295.
[41] Huang Y.Y., Ahir S., Terentjev E., Dispersion rheology of carbon nanotubes in a polymer matrix. Phys. Rev. B., 2006, 73(12), 1-9.
[42] Barbhuiya S., Chow P.. Nanoscaled Mechanical Properties of Cement Composites Reinforced with Carbon Nanofibers, Materials, 2017, 10(6), 662-672.
[43] Galao O., Baeza F.J., Zornoza E., Garcés P., Strain and damage sensing properties on multifunctional cement composites with CNF admixture, Cem. Concr. Compos., 2014, 46, 90-98.
[44] Shamsaei E., de Souza F.B., Yao X.P., Benhelal E., Akbari A., Duan W.H. Graphene-based nanosheets for stronger and more durable concrete: A review, Constr. Build. Mater., 2018, 183, 642-660.
[45] Chen S.J., Li C.Y., Wang Q., Duan W.H., Reinforcing mechanism of graphene at atomic level: Friction, crack surface adhesion and 2D geometry, Carbon, 2017, 114, 557-565.
[46] Lu Z.Y., Hou D.S., Ma H.Y., Fan T.Y., Li Z.J., Effects of graphene oxide on the properties and microstructures of the magnesium potassium phosphate cement paste, Constr. Build. Mater., 2016, 119, 107-112.
[47] Pan Z., He L., Qiu L., Korayem A.H., Li G., Zhu J.W., Collins F., Li D., Duan W.H., Wang M.C., Mechanical properties and microstructure of a graphene oxide–cement composite, Cem. Concr. Compos., 2015, 58 140-147.
[48] Gholampour A., Valizadeh K.M., Dnh T., Ozbakkaloglu T., Losic D., From Graphene Oxide to Reduced Graphene Oxide: Impact on the Physiochemical and Mechanical Properties of Graphene-Cement Composites, ACS Appl. Mater. Interfaces, 2017, 9(49), 43275-43286.
[49] Wang W., Chen S.J., Basquiroto de Souza F., Wu B., Duan W.H., Exfoliation and dispersion of boron nitride nanosheets to enhance ordinary Portland cement paste, Nanoscale, 2018, 10(3), 1004-1014.

Appendix

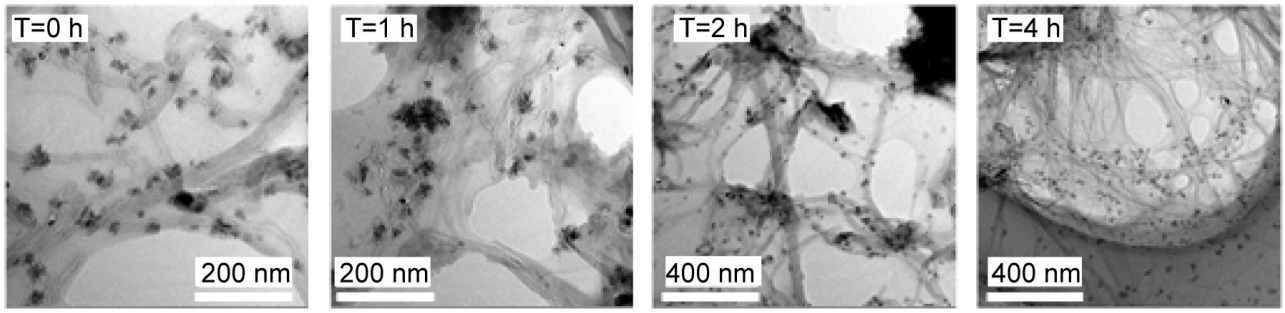

(a)

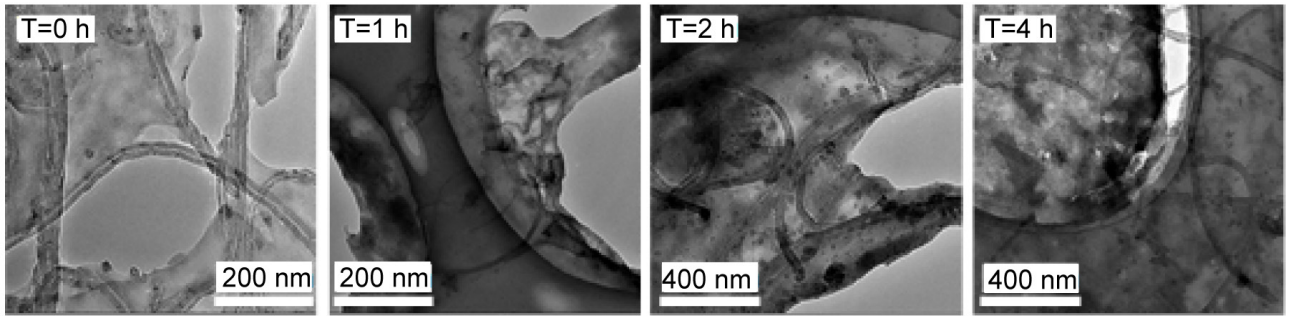

(b)

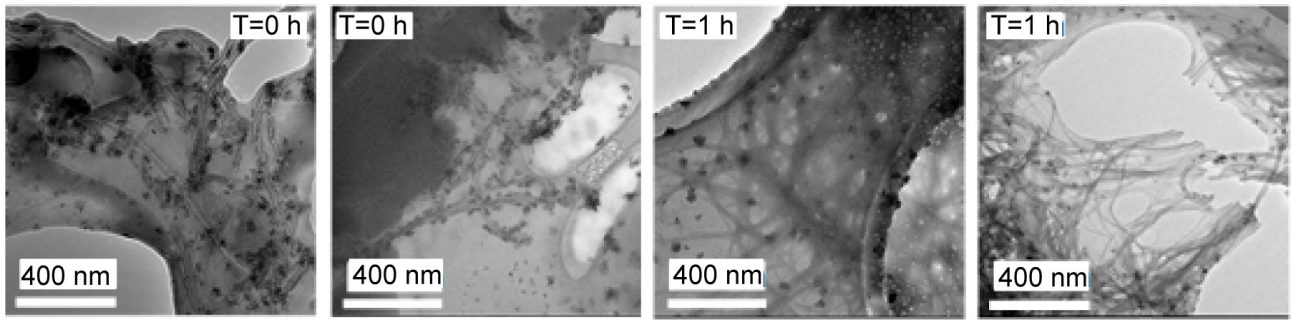

(c)

Figure S1

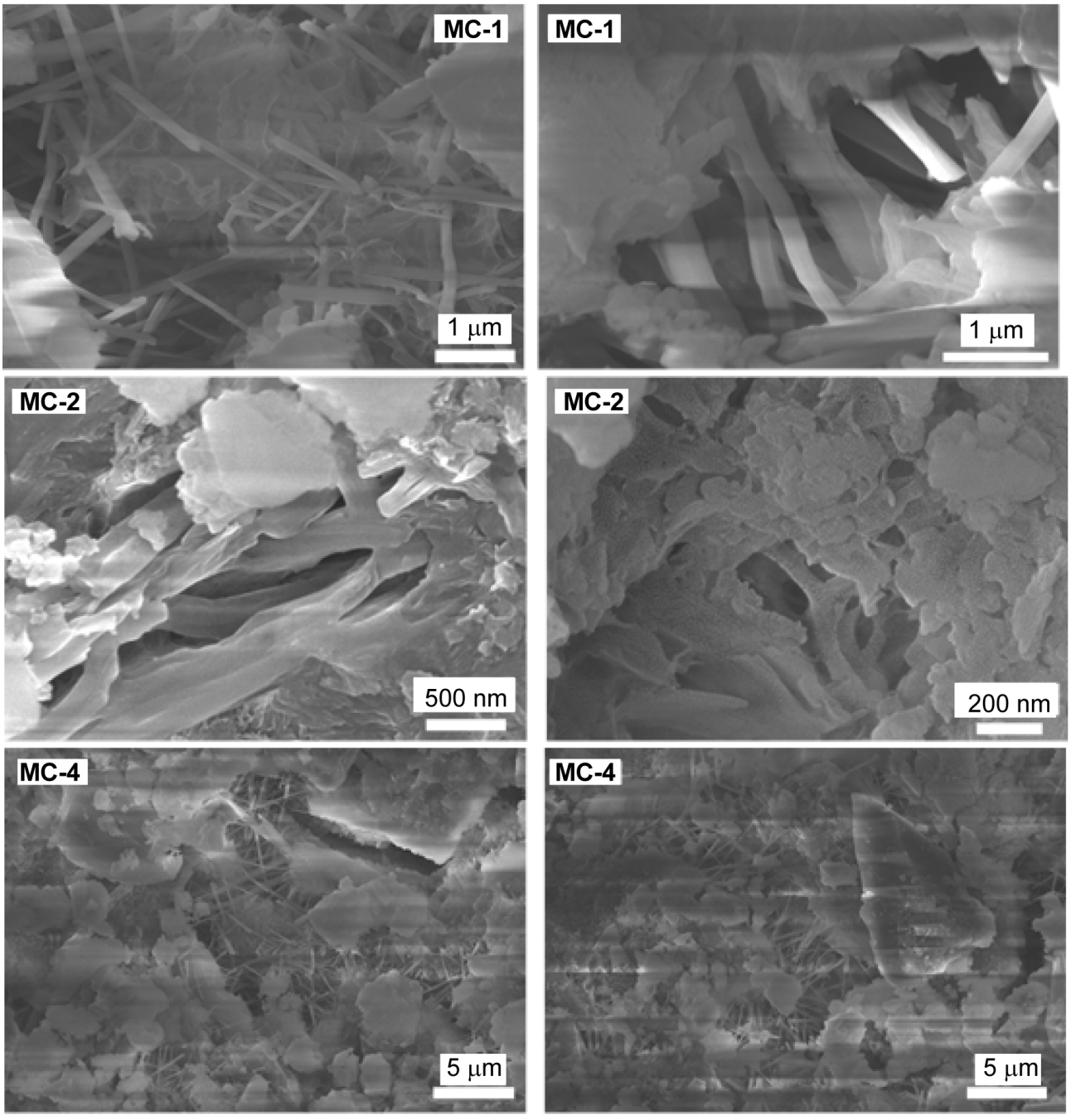

Figure S2